Spatial transcriptomics identifies spatially dysregulated expression of GRM3 and USP47 in amyotrophic lateral sclerosis

Spatial transcriptomics identifies spatially dysregulated expression of *GRM3* and *USP47* in amyotrophic lateral sclerosis

J. M. Gregory*†‡, K. McDade*†‡, M. R. Livesey‡§, I. Croy†¶, S. Marion de Proce¶, T. Aitman‡¶, S. Chandran*‡§ and C. Smith*†‡

*Centre for Clinical Brain Sciences, University of Edinburgh, †Edinburgh Pathology, University of Edinburgh, ‡Euan MacDonald Centre for Motor Neurone Disease Research, University of Edinburgh, §Centre for Discovery Brain Sciences, University of Edinburgh and ¶Centre for Genomic and Experimental Medicine, Institute of Genetics and Molecular Medicine, University of Edinburgh, Edinburgh, UK

J. M. Gregory, K. McDade, M. R. Livesey, I. Croy, S. Marion de Proce, T. Aitman, S. Chandran and C. Smith (2020) *Neuropathology and Applied Neurobiology* **Spatial transcriptomics identifies spatially dysregulated expression of *GRM3* and *USP47* in amyotrophic lateral sclerosis**

Aims: The mechanisms underlying the selective degeneration of motor neurones in amyotrophic lateral sclerosis (ALS) are poorly understood. The aim of this study was to implement spatially resolved RNA sequencing in human *post mortem* cortical tissue from an ALS patient harbouring the *C9orf72* hexanucleotide repeat expansion to identify dysregulated transcripts that may account for differential vulnerabilities of distinct (i) cell types and (ii) brain regions in the pathogenesis of ALS. **Methods**: Using spatial transcriptomics (ST) we analysed the transcriptome of *post mortem* brain tissue, with spatial resolution down to 100 μm. Validation of these findings was then performed using BaseScope, an adapted, *in situ* hybridization technique with single-transcript single-cell-resolution, providing extensive regional and cell-type specific confirmation of these dysregulated transcripts. The validation cohort was then extended to include multiple *post mortem* brain regions and spinal cord tissue from an extended cohort of *C9orf72*, sporadic ALS (sALS) and *SOD1* ALS cases. **Results**: We identified sixteen dysregulated transcripts of proteins that have roles within six disease-related pathways. Furthermore, these complementary molecular pathology techniques converged to identify two spatially dysregulated transcripts, *GRM3* and *USP47*, that are commonly dysregulated across sALS, *SOD1* and *C9orf72* cases alike. **Conclusions**: This study presents the first description of ST in human *post mortem* cortical tissue from an ALS patient harbouring the *C9orf72* hexanucleotide repeat expansion. These data taken together highlight the importance of preserving spatial resolution, facilitating the identification of genes whose dysregulation may in part underlie regional susceptibilities to ALS, crucially highlighting potential therapeutic and diagnostic targets.

Keywords: amyotrophic lateral sclerosis, BaseScope, molecular pathology, *post mortem*, spatial transcriptomics

Introduction

Genetics can influence the development of amyotrophic lateral sclerosis (ALS), with both causative genes in familial cases (fALS) and an increasing number of susceptibility genes. fALS cases make up approximately 10–20% of all cases of ALS and over a dozen causative genes have been described [1,2]. The recently identified intronic hexanucleotide repeat expansion in chromosome 9 open reading frame 72 (*C9orf72*) accounts for 40–50% of fALS [3,4]. Carrying and ubiquitously

*Correspondence: Jenna M. Gregory and Colin Smith, Centre for Clinical Brain Sciences, University of Edinburgh, Chancellor's Building, Edinburgh EH16 4SB, UK. Tel: +44 0131 465 9519; E-mail: jgregor2@ed.ac.uk and col.smith@ed.ac.uk

expressing this repeat expansion is thought to result in neurotoxicity and cell death contributing to the clinical manifestations of ALS through three putative mechanisms: (i) repeat-associated non-AUG (RAN)-translation of the hexanucleotide repeat, resulting in five highly aggregation-prone dipeptide repeat proteins, whose pathological accumulation is thought to cause proteotoxic stress, cytotoxicity and may lead to the sequestration of other aggregation-prone proteins [5], (ii) pathological formation of RNA foci, potentially sequestering functional RNA transcripts and RNA/DNA-binding proteins preventing their normal function [6] and (iii) loss of normal C9orf72 protein function due to haploinsufficiency resulting from the repeat expansion inhibiting normal protein production [7]. However, there is considerable heterogeneity in the penetrance and clinical manifestations of the *C9orf72* repeat expansion mutation, where patients who carry the same mutation present with diverse symptoms that span an ALS-frontotemporal dementia (FTD) spectrum [8]. This considerable clinical heterogeneity presents a substantial diagnostic challenge and makes stratification of ALS patients in clinical trials very difficult. However, despite this clinical heterogeneity there are shared pathological pathways in ALS pathogenesis [9].

TDP-43 is an RNA/DNA-binding protein involved in transcriptional regulation and is found at *post mortem* in the majority of ALS cases to be misfolded and accumulated as cytoplasmic aggregates [10]. The pathological misfolding of TDP-43 is thought to contribute to neurotoxicity through two major pathways: (i) gain of function, due to the presence of toxic aggregates in the cytoplasm that have the ability to sequester other aggregation-prone proteins and impair the balance of proteostasis in the cell and (ii) loss of function, whereby the normally nuclear TDP-43 is sequestered in cytoplasmic aggregates and is no longer able to participate in transcriptional regulation [9]. Clearly, given the common neuropathological finding of TDP-43 aggregates in central nervous system (CNS) tissue at *post mortem* in a majority of ALS cases, transcriptional dysregulation resulting from TDP-43 loss of function is an important mechanism warranting further investigation. Importantly, once thought of as purely a disorder of motor neurones, ALS is now recognized as showing a complex interplay between neurones and glia [11]. Indeed, glial TDP-43 inclusions are seen in cases of ALS and FTD, and there is evidence supporting active neuroanatomical propagation of molecular processes [12].

RNA sequencing allows transcriptional information to be analysed from ALS patients and compared with control tissue to highlight key pathways involved in the pathological disease process. Currently, RNA sequencing studies use whole-tissue homogenates of specific brain regions and cannot provide *in situ* information at a cellular level regarding the complex relationship between different cell types due to the lack of spatial resolution. A recently developed technique, called spatial transcriptomics (ST), has been developed that modifies RNA sequencing methodology to allow interrogation of the entire transcriptome while retaining *in situ* spatial information [13]. This technique has been successfully implemented in ALS mouse models and human spinal cord tissue [14].

Post mortem CNS tissue is subject to high levels of autolysis and ALS CNS tissue is particularly vulnerable to these *post mortem* changes as patients often die in an acidotic state due to agonal respiratory failure. We therefore chose to examine an area of the brain, the cerebellum, that is better preserved at *post mortem* compared to other brain regions [15] and only selected tissue with an RNA integrity number (RIN) of greater than 6. The additional benefit of examining the cerebellum is that, in ALS patients carrying the *C9orf72* hexanucleotide repeat, there is a high burden of protein misfolding without the corresponding cell death that is seen in other brain areas [16]. This is particularly useful when examining transcriptional dysregulation because in brain areas with substantial cell death, for example in the motor cortex, there will be a number of transcripts whose dysregulation is simply related to cell death and is not related to active disease processes. Our aim in this study is therefore to initially examine the cerebellum to circumvent this 'dying-cell artefact' and then validate any potential candidate transcripts in other brain regions using a complementary technique, BaseScope. By assessing only the granule cell layer of the cerebellum (substantial pathology with no associated cell death), this approach enables us to focus on transcripts associated with active disease rather than artefacts of dying tissue.

This is, to our knowledge, the first known application of this technology to deeply phenotyped human *C9orf72* ALS cortical tissue with a unique approach to circumvent dying-cell artefact. Furthermore, due to

limitations in the spatial resolution of ST (100 μm), we implemented, in parallel, a complementary technique called BaseScope, as a targeted approach with single-transcript, single-cell resolution [17]. Taken together these techniques have allowed us to interrogate the previously unexplored, spatial transcriptome of human *post mortem* ALS CNS tissue.

The aim of this study was to detect and spatially resolve transcriptional differences between brain regions and their composite cell types in ALS patient neural tissue compared to control tissue, to identify underlying differential cell vulnerabilities to the disease process in ALS, ultimately to inform therapeutic target selection and biomarker development in this field.

Experimental procedures

Case and tissue selection

All clinical data were collected as part of the Scottish Motor Neurone Disease register (ethics approval from Scotland A Research Ethics Committee 10/MRE00/78 and 15/SS/0216) and all patients consented to the use of their data during life. All *post mortem* tissue was collected via the MRC Edinburgh Brain Bank (East of Scotland Research Ethics Services [EoSRES] LR/16/ES/0084). Use of human tissue for *post mortem* studies has been reviewed and approved by the Edinburgh Brain Bank ethics committee and the Academic and Clinical Central Office for Research and Development (ACCORD) medical research ethics committee (AMREC). Cases had all undergone whole genome sequencing and repeat-prime PCR (for *C9orf72* hexanucleotide repeat expansion) to identify genetic diagnoses.

Control cases were age-matched and had no neurological disease during life and no significant neuropathology identified at *post mortem* examination.

Spatial transcriptomics

For a detailed explanation of how the spatial transcriptomics technology works please see the manufacturers website: https://www.10xgenomics.com/spatial-transcriptomics/?creative=368028668309&keyword=spatial%20transcriptomics&matchtype=p&network=g&device=c&gclxml:id=CjwKCAjwtO7qBRBQEiwAl5WC28N14goS4HgrNresRYl_j3JZvmfGA2Cn7cne8rKc9wzKSbSDlV1IIBoC84cQAvD_BwE.

The RNA integrity number (RIN) of the tissues used was ALS: 6.2 and Control: 6.8. A block of brain tissue was cut to an appropriate size, approximately 5–7 mm^2 and sections were cut on a cryostat set to −20°C at 10 μm thickness on to the commercially available library preparation ST slides within the pre-specified areas containing the mRNA probes (six areas per slide). One area was left blank as a negative control. Once cut, slides and sectioned tissue were stored at −80°C. All subsequent work was carried out inside a clean laminar flow hood. The slide was heated for 1 min at 37°C. Nine hundred microlitres of freshly diluted 4% paraformaldehyde was added to the surface of the slide ensuring all tissue was covered and incubated at room temperature for 10 min. The slide was then washed by dipping in to 1× PBS (phosphate buffered saline) five times followed by incubation in 500 μl isopropanol for 1 min and the slide was then air-dried. Haematoxylin and eosin (H&E) staining was performed by firstly incubating sections in 500 μl Harris haematoxylin (ThermoFisher) for 4 min and washed by dipping 10 times in RNAase/DNAase free water and 1 dip in acid alcohol (1 % HCl in 70 % ethanol) followed by 10 further dips in RNAase/DNAase free water. Sections were then incubated in 500 μl of bluing buffer (Dako) for 30 sec followed by dipping 10 times in RNAase/DNAase free water. Sections were then incubated in 500 μl of Eosin Y (ThermoFisher) for 4 min followed by dipping 10 times in RNAase/DNAase free water. Slides were then air-dried and incubated at 37°C for 5 min and mounted with a coverslip using 100 μl of 85% glycerol. The slide was then imaged at 40× magnification. The remainder of the procedure was done as previously reported [13]. In brief, following removal of the coverslip, prepermeabilization (5-min incubation) and permeabilization (10-min incubation) was performed using pepsin and collagenase, followed by cDNA synthesis and probe cleavage on the slide. Samples collected following probe cleavage were then processed as per library preparation protocol published previously [13] to prepare the probe-mRNA construct for sequencing (involving the addition of the Illumina adapter (read 2) and the third unique molecular identifier (UMI), the array ID). The finished libraries then underwent quality control by assessing integrity and concentration by bioanalyser analysis (high sensitivity chip) and qubit analysis. Following this, four libraries (2 × ALS and 2 × control) were submitted to

Edinburgh Genomics for 75 paired end sequencing over 1 lane of a flow cell as 1 pooled library on the HiSeq 4000 platform. Sequences were analysed as detailed in the ST pipeline ([18]; an automated pipeline for spatial mapping of unique transcripts Oxford BioInformatics 10.1093/bioinformatics/btx211). In brief, fastq files for paired reads (read 1 and read 2) were decoupled using their unique well IDs. Analysis firstly involved quality trimming by removing reads with low quality bases and low quality UMIs, removing artefacts and checking AT and GC content. The reads were then mapped to the human reference genome version 89 using STAR software, demultiplexed (removing duplicate reads) using Taggd software and then individual reads were annotated using htseq-count and group annotated by barcode (spot position), gene and genomic location to obtain the read count [18]. The final output included the gene name, read count and spot position in a format that was directly uploaded to the ST viewer software [18] for integration with the two high-resolution images (i) H&E (tissue morphology) and (ii) Cy3 spots (location of transcripts) for spatial analysis. Following this, spatial analysis was performed using the ST viewer software according to the user manual [18]. Spots underlying the granule cell layer were selected based on cell morphology determined by H&E image (spots highlighted by white circles in Figure 1**B**), spots on the edge of each region were excluded from the analysis, to reduce bias. Analysis was performed in ST viewer comparing the most differentially expressed transcripts based on predetermined spot selections. NB: we only selected spots directly underlying tissue and QC data are presented in Table S2.

Immunohistochemistry

p62 staining was performed on serial sections of frozen brain tissue cut at the same time, same temperature and same thickness as ST sections. Sections were placed in a slide holder in running tap water to remove OCT and washed in Tris buffered saline (TBS) for 5 min followed by incubation with mouse-anti-p62 primary antibody (BDbio-610833 150 ug LCK ligand) at a 1 in 1000 dilution in TBS overnight at room temperature. Antibody detection was then performed using Novolink max polymer detection kit. A 5-min wash with TBS was followed by a post primary blocking step for 30 min at room temperature, followed by a 5-min wash with TBS and incubation with Novolink polymer for 30 min at room temperature. A TBS wash for 5 min was then followed by incubation with 3, 3′ diaminobenzidine tetrahydrochloride (DAB) (50 l chromogen + 1 ml DAB substrate buffer) for 5 min followed by washing in running water for a further 2 min. The sections were then counterstained with Harris haematoxylin for 1 min followed by dipping in lithium carbonate for 30 sec, then a dip in each of 70% ethanol and xylene and mounted with a 24 × 50 mm coverslip using two drops of VectaMount mounting medium. Sections were then imaged at 20 × magnification on a NanoZoomer.

BaseScope

For a detailed explanation of how the BaseScope technology works please see the manufacturer's website: https://acdbio.com/science/how-it-works.

Brain tissue was taken at *post mortem* from standardized Brodmann areas (BA) and fixed in 10% formalin for a minimum of 24 h. Tissue was dehydrated in an ascending alcohol series (70–100%) followed by three successive 4-h washes in xylene. Three successive 5-h paraffin wax embedding stages were performed followed by cooling and sectioning of the FFPE (formalin-fixed paraffin embedded) tissue on a Leica microtome in 4 μm sections on to a superfrost microscope slide. BaseScope reagents (*Advanced Cell Diagnostics*) were used as per manufacturer's guidelines according to the original protocol [17]. In brief, following deparafinization, tissue sections were incubated with hydrogen peroxide for 10 min at room temperature and target antigen retrieval was performed by submerging slides in BaseScope 1X target retrieval reagent at 99°C in a Braun Multiquick FS 20 steamer for 15 min. The tissue was then permeabilized using BaseScope protease III at 40°C for 30 min. Probe hybridization was then performed by incubating the slides with four drops of custom designed BaseScope probe, negative control probe (DapB) or positive control (PPIB) probe for 2 h at 40°C. Following successive probe amplification steps, transcripts were detected using the BaseScope RED detection kit and slides were counterstained using haematoxylin and lithium carbonate. The slides were then cleared in xylene and mounted with a 24 × 50 mm coverslip using two drops of VectaMount mounting medium. Sections were then imaged at

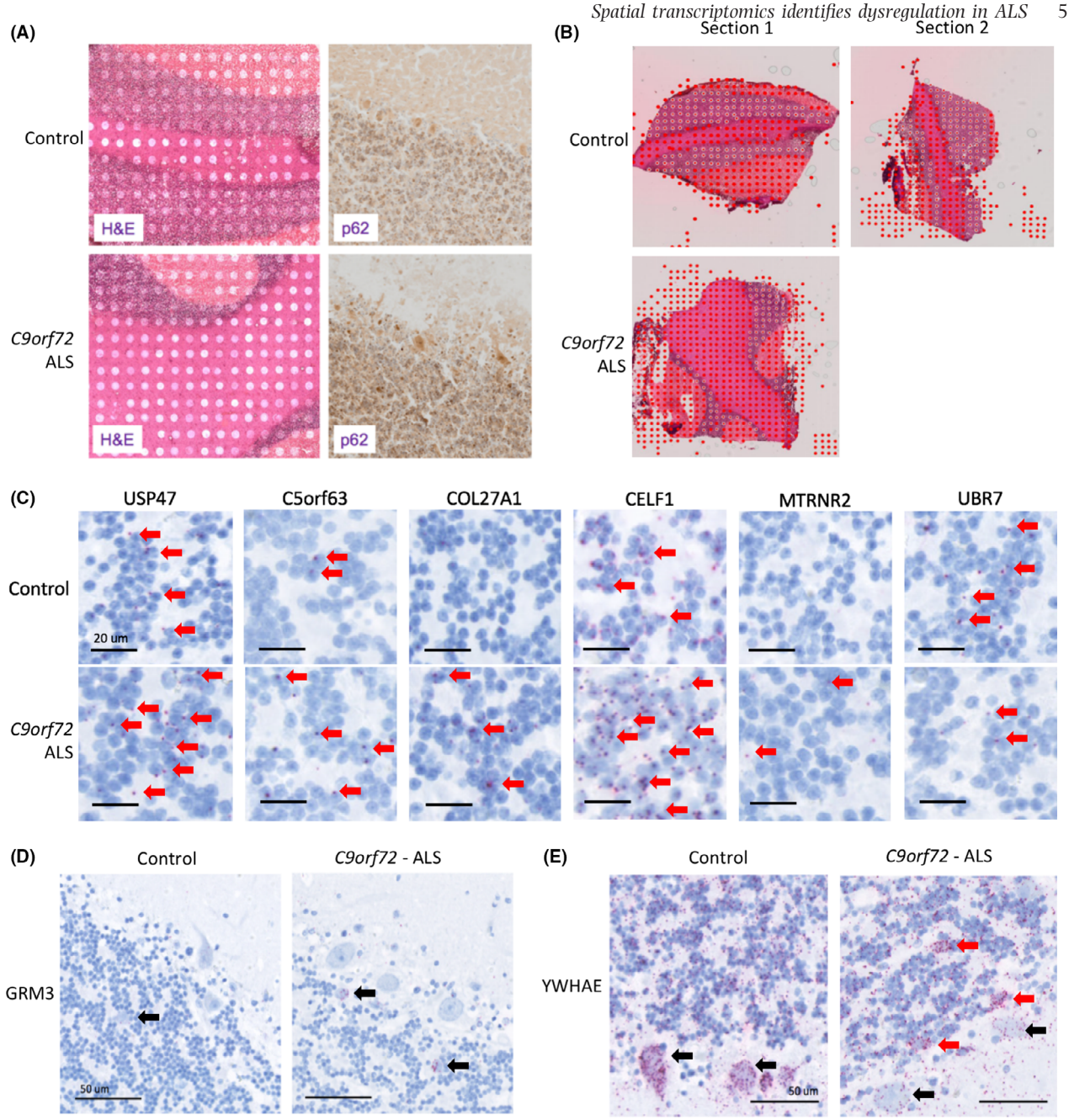

Figure 1. Spatial transcriptomics identifies 16 candidate transcripts with dysregulated expression in cerebellum of ALS *C9orf72* patient. (**A**) Left panels: haematoxylin and eosin (H&E) stained sections of cerebellum (above: control tissue and below: *C9orf72* - ALS tissue) with Cy3 hybridization highlighting the spatial transcriptomics localization spots (pseudocoloured white) underlying the tissue. Right panels: serial sections immuno-stained with anti-p62 antibody highlighting p62-positive aggregates within the granule cell layer of the cerebellum of *C9orf72* - ALS tissue, but not control tissue. Scale: white dot diameter = 100 μm diameter. (**B**) H&E stained sections of cerebellum of the two control sections and one *C9orf72* - ALS section used in the ST analysis. Spots highlighted with white rings are the spots selected for analysis of the granule cell layer. Scale: dot diameter = 100 μm diameter. (**C**) BaseScope identification of single transcripts (1 red dot = 1 single transcript) within the granule cells of the cerebellum, counterstained with haematoxylin. Top panels: control tissue, bottom panels: *C9orf72* - ALS tissue (red arrows indicated single mRNA transcripts). Scale bar = 20 μm. (**D**) Sections of cerebellum counterstained with haematoxylin showing cell-type specific expression (1 single red dot = 1 single transcript) of *GRM3*, identified by BaseScope in the interneurons of the cerebellum, with increased expression in the interneurons (black arrows) of the *C9orf72* - ALS case compared to controls. Scale bar = 50 μm. (**E**) Sections of cerebellum counterstained with haematoxylin showing cell-type specific expression of *YWHAE*, identified by BaseScope in the interneurons (red arrows) and Purkinje cells (black arrows) of the cerebellum, with increased expression in the interneurons of the *C9orf72* - ALS case compared to increased expression within the Purkinje cells in the controls. Scale bar = 50 μm.

20 × magnification on a NanoZoomer slide scanner and the number of transcripts per cell was quantified by two independent pathologists.

Statistics

Differential expression was defined as >3-fold difference in expression (median number of transcripts identified per feature) between ALS and control tissue, but not between technical replicates of control tissue. Any transcripts where the overall read count was zero were excluded, to limit zero-inflation, as it is not possible to say whether this was because (i) there was no expression of that gene in that selection, or (ii) whether there was insufficient coverage to detect it or (iii) whether there has been degradation of the transcript. Therefore, transcripts were included as potential hits if they (i) reached statistical significance (compared to control expression), (ii) had a median number of transcripts per feature not equal to zero and (iii) had a greater than 3-fold difference between case and control expression. Due to the extensive nature of our planned validation cohort (multiple brain regions and multiple ALS cases including sporadic ALS (sALS), *SOD1* and additional *C9orf72* cases), this strict filtering process was performed to enable the greatest confidence in selecting a manageable number of high-value candidate transcripts. Median number of transcripts per feature was calculated by the ST software as stated above, data were not normally distributed and therefore significance was calculated by nonparametric testing using Mann-Whitney *U* test.

For BaseScope analysis, gene expression was calculated by counting the number of transcripts per cell in three randomly generated fields of view (1 mm^2) and then averaged. This was done for each of the twelve cases (three C9orf72 cases, three control cases, three sALS cases and three SOD1 cases) and the mean and standard deviation was plotted for each of the groups. Therefore, each group (Control, C9orf72, sALS and SOD1) plotted on the graph is the mean and standard deviation of three fields of view in three individuals. Differences in expression (number of dots/transcripts per cell; measured by BaseScope) between ALS case and control in Figure 1 were assessed by two-tailed unpaired t-tests following log transformation (x' = log

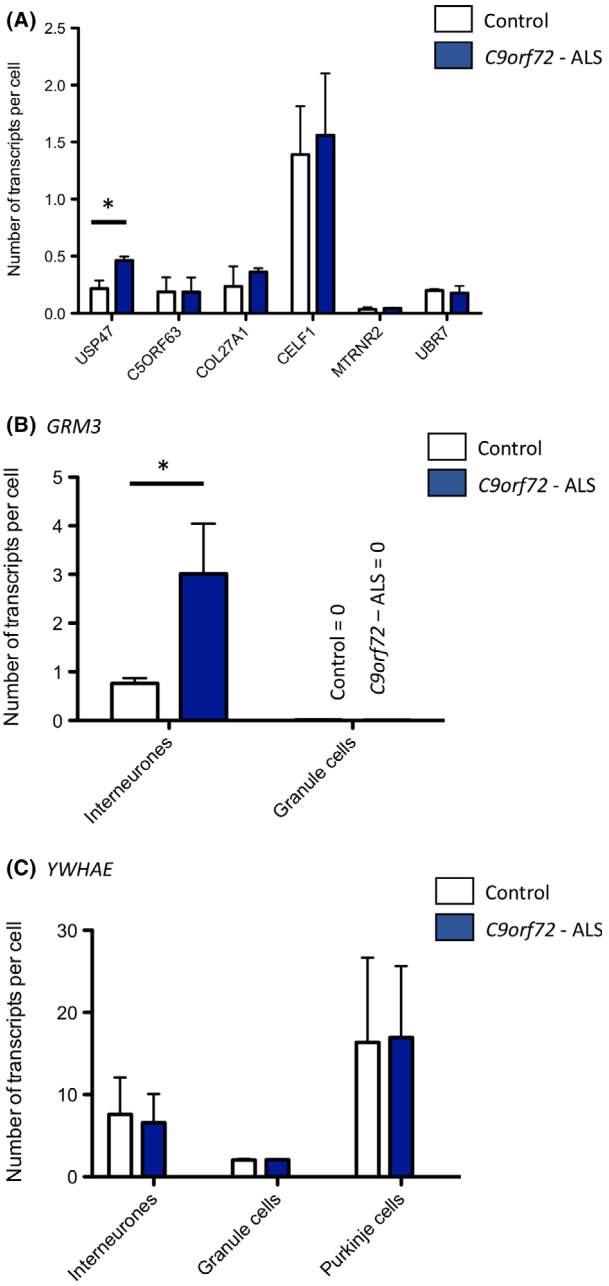

Figure 2. Spatial dysregulation of *GRM3* and *USP47* in cerebellum of an extended cohort of ALS *C9orf72* patients. (**A**–Table summarizing the clinical data associated with the *C9orf72* case selected for spatial transcriptomics evaluation.) Graphs quantifying expression of transcripts (measured by BaseScope) in three additional *C9orf72* cases and three additional control cases, demonstrating that only *USP47* (**A**) and *GRM3* (**B**) are consistently dysregulated in all cases, whereas spatial differences in *YWHAE* expression do not reach statistical significance (**C**). Error bars indicate standard deviation.

x + 1). Differences in expression in Figures 2–4 and Figure S2 were analysed using 1-way ANOVA (following log transformation), compared to control expression using a Bonferroni post-test correction for multiple testing.

Results

ST analysis identified 16 candidate transcripts with spatially dysregulated expression

Spatial transcriptomics analysis was performed on frozen sections of cerebellum from one ALS and one age- and sex-matched control case (Figure 1**A** and **B**). A summary of the clinical data of this case is included in Table 1. Serial sections were stained for p62 to demonstrate that there was evidence of substantial protein aggregation in the granule cell layer of the cerebellum of the ALS case, but not in the control case (Figure 1**A**; right panel). Initially, as a quality control (QC) exercise to test the ST analysis pipeline and software, to ensure that the images and transcripts were correctly aligned and that ST analysis can distinguish between different regions of the cerebellum, two QC experiments were performed. The first assessed four spatially conserved transcripts, known to be differentially expressed in each of the granule cell layer, molecular cell layer, Purkinje cells and white matter, were analysed and visualized as a heat map of expression. Spatial transcript expression analysis in this way demonstrated accurate regional specificity (Figure S1). The second QC experiment involved simulation of a whole-tissue RNA sequencing experiment and subsequent comparison of our data to a previously published whole-tissue data set. A transcriptomic analysis of *post mortem* whole-tissue from the cerebellum of patients carrying the *C9orf72* hexanucleotide repeat expansion was conducted previously, identifying 15 genes that were dysregulated between *C9orf72* tissue and control tissue [19]. Comparison of the entire section of our tissue, simulating a whole-tissue experiment, revealed that five of the 15 dysregulated transcripts detected in this previous study were replicated in our analysis (*ALAS2, HSPH1, DNAJB1, HSPA1A* and *HSPA1B;* Table S1).

Following these QC experiments, ST analysis was performed comparing control and ALS granule cell layers to identify candidate transcripts that may be differentially expressed accounting for differential vulnerabilities to disease. Only the spots underlying the granule cell layer (spots selected with a white circle; Figure 1**B**) were included in the analysis. The number of expressed genes identified in each of the sections ranged from 1123 in the ALS tissue and up to 2588 in the control tissue (summary of QC data is presented in Table S2). The number of genes identified was lower than expected, however is in line with other transcriptome analyses done in *post mortem* ALS CNS tissue [14]. This has been hypothesized to be a result of *post mortem* autolysis, which primarily affects 3' and 5' ends of the mRNA, affecting the 3' poly-A tag, crucial to the mRNA capture prior to sequencing.

Spatial analysis followed by the strict filtering process resulted in the identification of 16 differentially expressed candidate transcripts ([13] with a higher expression in ALS and 3 with a lower expression) in the granule cell layer of *post mortem* ALS patient cerebellum (Table 2). Gene ontology (GO) analysis was performed using *pantherdb.org* to identify common disease pathways between the identified transcripts. This analysis identified six prominent pathways: (i) proteostasis, (ii) RNA/DNA-binding proteins, (iii) mitochondrial metabolism, (iv) extracellular matrix, (v) excitotoxicity and (vi) apoptosis.

BaseScope analysis validated eight candidate transcripts and demonstrated highly specific spatially dysregulated expression

Given the limitations, primarily in coverage, of ST in our tissue we sought to validate the ST data using a complementary technique, BaseScope, which has high sensitivity and specificity for detection of transcripts on a single-cell level in histological sections. Using this technique, we assessed whether any of the sixteen transcripts identified by ST were dysregulated in the same case and control tissues as those used in the ST experiment. A summary of the clinical data of all cases used in for BaseScope validation is included in Table 3. BaseScope analysis showed independent evidence of differential expression for eight of the sixteen transcripts (*USP47, C5orf63, COL27A1, CELF1, MTRNR2, UBR7, GRM3 and YWHAE*; Figure 1**C**–**E**). Differential expression was not confirmed for the remaining eight transcripts (Figure S2). Furthermore, the added value of retaining spatial resolution was clearly highlighted by the identification of two transcripts (*GRM3* and

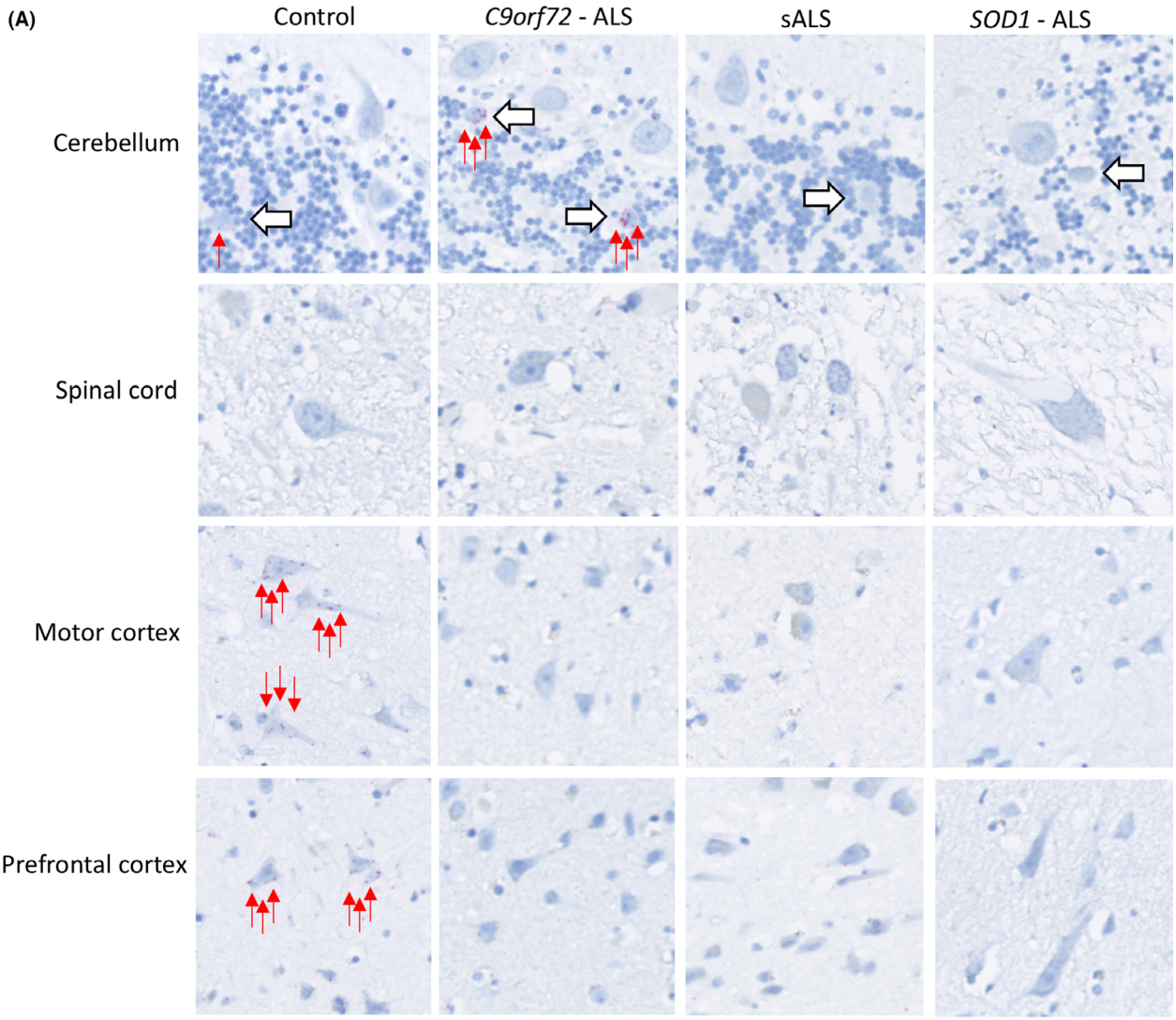

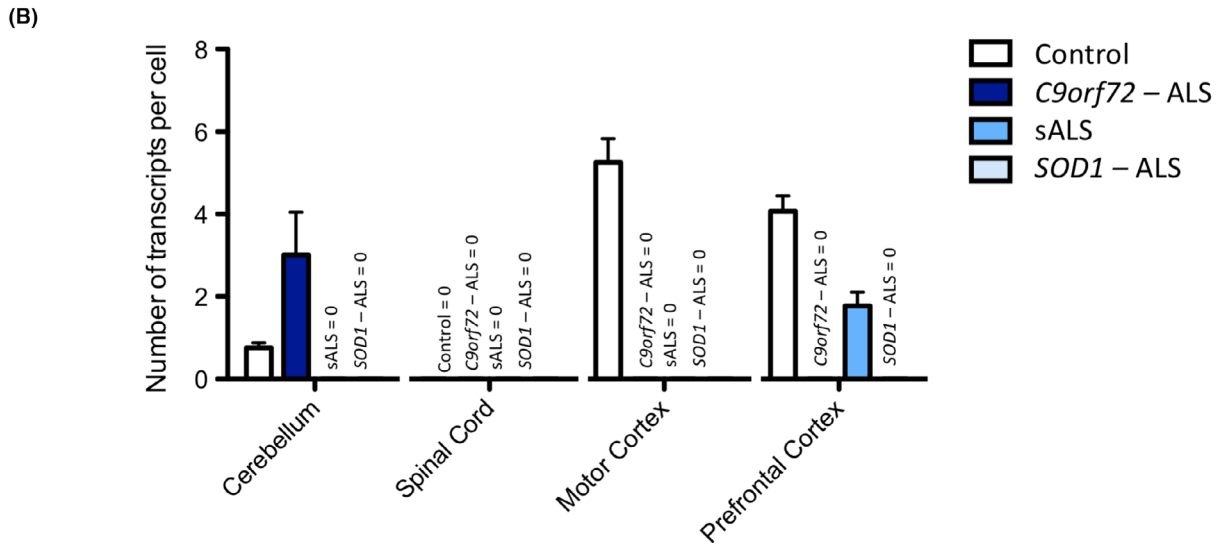

Figure 3. Expression of *GRM3* is downregulated globally in the cortex of ALS cases. (**A**) Representative images showing BaseScope identification of single transcripts (1 red dot = 1 single transcript) within the cerebellum, spinal cord, motor cortex and prefrontal cortex of brains of control, *C9orf72*, sALS and *SOD1* patients. Images demonstrate localization of transcripts of *GRM3* within the interneurons of the cerebellum (white arrows) and global cortical downregulation of *GRM3* in ALS cases compared to control cases. There is no expression of *GRM3* evident in the spinal cord of controls or ALS cases. Sections are counterstained with haematoxylin. (**B**) Graph quantifying expression of *GRM3* transcripts imaged in **A** in three control cases, three *C9orf72* cases, three sALS cases and three *SOD1* cases. Error bars indicate standard deviation.

YWHAE), whose expression was highly specifically dysregulated in *C9orf72* cerebellum compared to control cerebellum (Figure 1D and E). The expression of *GRM3* is restricted to the interneurones of the granule cell layer and is markedly increased in ALS granule cell interneurones compared to control interneurones in this layer (Figures 1**D** and 2**B**). The expression of *YWHAE* is also spatially dysregulated. Its expression is extensive within the cerebellum, however in control tissue it is predominantly expressed in the granule cells and the Purkinje cells, whereas in the ALS *C9orf72* case its expression is strikingly redistributed from the Purkinje cells to the interneurons of the granule cell layer (Figure 1**E**). It is highly unlikely that these transcriptional variations would have been identified using a whole-tissue approach or indeed without the retention of spatial resolution.

Spatial dysregulation of GRM3 and USP47 in cerebellum of an extended cohort of ALS C9orf72 patients

Due to cost of the existing ST technologies we had assessed only a single *C9orf72* case against a control case, but we sought to validate our observations across an increased number of *C9orf72* cases by using BaseScope. We validated the eight candidate transcripts across an additional three *C9orf72* cases with an additional three appropriately matched control cases. This analysis revealed that there were two candidate transcripts whose expression was consistently dysregulated in the cerebellum of all three *C9orf72* cases compared to the controls: *USP47* (Figure 2**A**) and *GRM3* (Figure 2**B**). The mean expression of *USP47* in the granule cells of the cerebellum of *C9orf72* patients was statistically significantly higher than that of control cases ($P = 0.005$; $t = 5.459$; df = 4). Furthermore, expression of *GRM3* in the cerebellar interneurones of ALS *C9orf72* cases was found to be over three times that of control interneurones ($P = 0.0204$; $t = 3.724$; df = 4). However, when the expression of *YWHAE* was examined across an extended cohort of *C9orf72* and control patients, the difference between *C9orf72* patients and control cases did not reach statistical significance (Figure 2**C**).

Extended CNS analysis reveals spatial dysregulation of GRM3 and USP47 in the cortex of diverse cohort of ALS patients

Given the consistent validation of *GRM3 and USP47* in an extended cohort of ALS *C9orf72* patients with two independent techniques (ST and BaseScope) we next sought to extend our transcriptional analysis of these two transcripts to additional brain regions and to other cases of ALS including three cases of *SOD1*-ALS and three cases of sALS compared to the three *C9orf72* cases and three controls. We assessed expression in the spinal cord, motor cortex, prefrontal cortex and cerebellum of all twelve cases (Figure 3). There was no expression of *GRM3* in the spinal cord of any of the cases (neither control nor ALS; Figure 3**A**). However, whilst the transcriptional dysregulation observed in the interneurons of the granule cell layer of the cerebellum was restricted to *C9orf72* cases, dysregulation of *GRM3* across the cerebral cortex was a phenomenon observed in all ALS cases (Figure 3**A**). Expression of *GRM3* in the motor cortex and prefrontal cortex was statistically significantly lower in the *C9orf72*, sALS and *SOD1* cases compared to controls (Figure 3**B**), despite showing no significant difference in positive and negative control genes (Figure S3). The expression of *USP47* was also found to be highly spatially dysregulated. Whilst the transcriptional dysregulation observed in the granule cells of the cerebellum was restricted to *C9orf72* cases, dysregulation of *USP47* across the cerebral cortex and spinal cord was observed in all ALS cases (Figure 4**A**). Expression of *USP47* in the spinal cord, motor cortex and prefrontal cortex was statistically significantly lower in the *C9orf72*, sALS and *SOD1* cases compared to controls (Figure 4**B**).

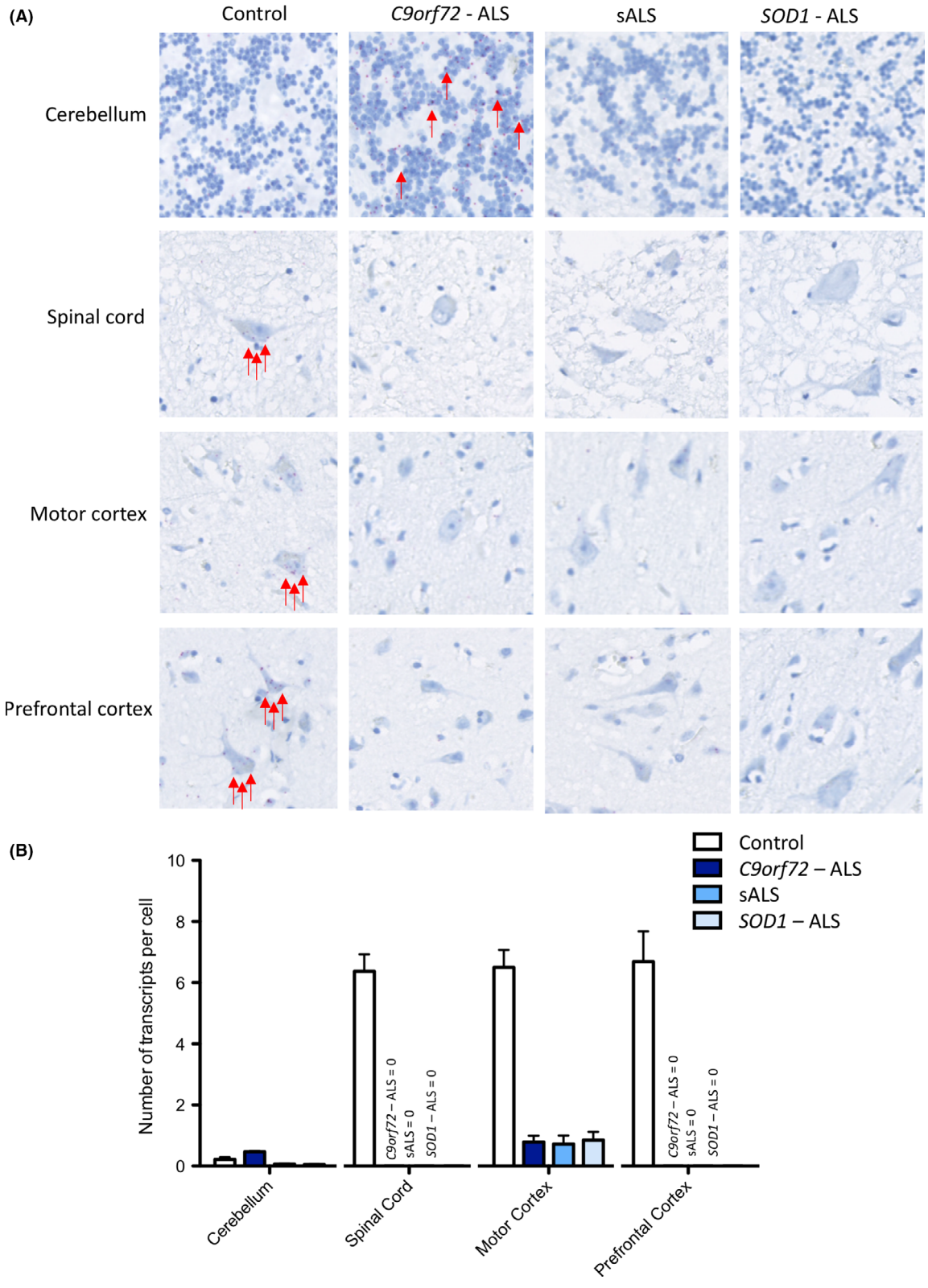

Figure 4. Expression of *USP47* is downregulated globally in the CNS of ALS cases. (**A**) Representative images showing BaseScope identification of single transcripts (1 red dot = 1 single transcript) within the cerebellum, spinal cord, motor cortex and prefrontal cortex of brains of control, *C9orf72*, sALS and *SOD1* patients. Images demonstrate localization of transcripts of *USP47* within the interneurons of the cerebellum (white arrows) and global cortical downregulation of *USP47* in ALS cases compared to control cases. There is no expression of *USP47* evident in the spinal cord of controls or ALS cases. Sections are counterstained with haematoxylin. (**B**) Graph quantifying expression of *USP47* transcripts imaged in **A** in three control cases, three *C9orf72* cases, three sALS cases and three *SOD1* cases. Error bars indicate standard deviation

Discussion

Spatial transcriptomics is a powerful tool in the analysis of (i) spatially heterogeneous tissues like the brain and (ii) spatially heterogeneous diseases, like ALS. Our ST analysis identified sixteen candidate dysregulated transcripts from six relevant disease-related pathways. Furthermore, the dysregulation of two of these transcripts, *GRM3* and *USP47*, was confirmed in an extensive cohort of ALS patients, including three sALS cases and three *SOD1* ALS cases (all harbouring the *p.I114T* Scottish founder mutation) in addition to three *C9orf72* ALS cases, all compared to three control cases, using a complementary technique, BaseScope.

GRM3 as a potential therapeutic target in ALS

Data in this study demonstrate that gene expression of *GRM3* is consistently lower in the prefrontal and motor cortex in *C9orf72* repeat expansion, mutant *SOD1* and sALS compared to controls. Furthermore, our data indicate divergence of *GRM3* expression between ALS subtypes, where specifically *GRM3* expression is higher in interneurones in the granule cell layer of the cerebellum in *C9orf72* repeat expansion patients.

Table 1. Summary of clinical data for C9orf72 case used in the spatial transcriptomics experiment

Age of onset	54
Age at death	62
Disease duration (months)	97
Sex	Female
El Escorial	3
Site of onset	Lower limb
Family history	Brother had MND
Genetics	*C9orf72* hexanucleotide repeat expansion identified by repeat prime PCR, no other abnormalities identified by whole genome sequencing.
Cognitive assessment	ECAS – Impaired (total ECAS score = 102; ALS-specific score = 76; impaired in executive and fluency tasks, but not in language tasks)
Summary of pathology	Brain weight 1220 g p62 in dentate gyrus, CA4 sector of hippocampus and granule cells of cerebellum Ventral nerve root atrophy throughout spinal cord

Table summarizing the clinical data associated with the *C9orf72* case selected for spatial transcriptomics evaluation.

The *GRM3* gene encodes $mGlu_3$, a metabotropic glutamate receptor known to modulate glutamate neurotransmission in the central nervous system. Data obtained from control tissue by this study are consistent with previous descriptions of the $mGlu_3$ receptor in human tissue; *GRM3* is expressed in neurons within the cerebral cortex, interneurons/Golgi cells in the cerebellum, but not in spinal cord neurons (reviewed in [20]). Neuronal $mGlu_3$ receptor expression is largely found at presynaptic terminals, though at extrasynaptic sites not associated with active synaptic zones. This appears to be inherently related to the physiological role of $mGlu_3$ receptors, where activation by extrasynaptic glutamate overspill negatively regulates presynaptic vesicular release of glutamate by modulation of presynaptic ion channel activity through G-protein signalling cascades [21–24]. The inhibition or decreased expression of $mGlu_3$ receptors is therefore consistent with an increased glutamate transmission and excitotoxic scenarios [25,26]. $mGlu_3$ receptors are also expressed in astrocytes and activation via synaptic glutamate or $mGlu_3$ agonists generate the release of neuroprotective neurotrophic factors in a rodent mutant SOD1 ALS model [26]. Of note, the reduction of $mGlu_3$ receptor expression in the prefrontal cortex is more commonly associated with neuropsychiatric diseases including schizophrenia and bipolar disorder [27,28]. These studies suggest there may be shared mechanistic features between schizophrenia and ALS [29]. In this regard, a common convergence of reduced $mGlu_3$ receptors in ALS and neuropsychiatric disease is potentially highlighted by the fact the $mGlu_3$ receptor knock out mouse was initially generated to understand neuropsychiatric disease, however, also displays locomotor dysfunction [30,31]. The development of selective pharmacology targeting $mGlu_3$ receptors in

Table 2. Table of dysregulated transcripts identified through ST analysis

Gene	*Fold increase in C9orf72 -* ALS	*P*-value	*Median read count in C9orf72 -* ALS	*BaseScope mean transcripts per cell in control* (*n* = 3)	*BaseScope mean transcripts per cell in C9orf72-ALS* (*n* = 3)	*P*-value	*Pathway*	*Gene info*
APP	3	<0.05	3	0.40	0.45	>0.05	Proteostasis	Signalling molecule
NFIB	3	<0.05	3	0.38	0.37	>0.05	RNA/DNA-binding	Nuclear factor 1 B-type
USP47	3	<0.05	3	0.22	0.46	>0.05	Proteostasis	De-ubiquitinating protein
ATP8	4	<0.05	4	Probe failed	Probe failed	N/A	Mitochondrial function	ATP synthase protein 8
C5orf63	4	<0.05	4	0.19	0.19	>0.05	Mitochondrial function	Glutaredoxin-like protein
COL27A1	4	<0.05	4	0.24	0.36	>0.05	Extracellular matrix	Collagen alpha-1 (XXVII) chain
ALG14	5	<0.05	5	0.03	0.04	>0.05	Proteostasis	ER N-glycosylation
FAM155A	5	<0.05	5	0.11	0.09	>0.05	Excitotoxicity	Calcium import
CELF1	5	<0.05	5	1.39	1.56	>0.05	RNA/DNA-binding	CUGBP Elav-like family
GRM3	5	<0.05	5	0.76	3.01	<0.05	Excitotoxicity	Metabotropic glutamate receptor
COX1	9	<0.05	18	Probe failed	Probe failed	N/A	Mitochondrial function	Cytochrome c oxidase subunit 1
MTRNR2	13	<0.05	23	0.03	0.04	>0.05	Anti-apoptotic	Neuroprotective/ anti-apoptotic
YWHAB	13	<0.05	36	0.29	0.30	>0.05	Proteostasis	Chaperone 14-3-3 protein beta/alpha

Gene	*Fold decrease in C9orf72 -* ALS	*P*-value	*Median read count in C9orf72 -* ALS	*BaseScope mean transcripts per cell in control* (*n* = 3)	*BaseScope mean transcripts per cell in C9orf72-ALS* (*n* = 3)	*P*-value	*Pathway*	*Gene info*
YWHAE	4	<0.05	1	7.59	6.57	>0.05	Proteostasis	Chaperone 14-3-3 protein epsilon
ZFR	3	<0.05	3	Probe failed	Probe failed	>0.05	RNA/DNA-binding	Zinc finger RNA-binding protein
UBR7	3	<0.05	1	0.20	0.18	>0.05	Proteostasis	Putative E3 ubiquitin-protein ligase

Upper panel of table displays information regarding the 13 transcripts that are upregulated in *C9orf72* ALS tissue compared to control tissue following filtering analysis. Lower panel displays information regarding the 3 transcripts that are down regulated in ALS tissue compared to control tissue following filtering analysis.

neuropsychiatric disease may also therefore be relevant to motor aspects of ALS.

USP47 and de-ubiquitinating proteins

As the granule cell layer in *C9orf72 post mortem* cerebellar tissue is subject to a high burden of protein misfolding [32], it is understandable that the pathway common to many of the candidate transcripts is proteostasis. The upregulation of proteostatic mechanisms such as chaperone proteins and the ubiquitin-proteasome system (UPS) to cope with the high levels of protein misfolding may enable these cells to survive despite a high burden of cytotoxic protein misfolding. The UPS is a pathway whereby cells can target unwanted or misfolded proteins for degradation by covalently linking them with ubiquitin molecules. This ubiquitin chain targets the client protein to the

Table 3. Summary of neuropathological assessment for additional *C9orf72* cases (evaluated in Figures 2–4)

	C9orf72 Case 1	*C9orf72 Case 2*	*C9orf72 Case 3*	*sALS case 1*	*sALS case 2*	*sALS case 3*	*SOD1 case 1*	*SOD1 case 2*	*SOD1 case 3*
Age of onset	60	54	51	46	59	55	59	32	71
Disease duration (months)	33	109	89	30	46	134	98	67	38
Sex	Female	Female	Male	Female	Male	Male	Female	Male	Male
Site of onset	Lower limb	Lower limb	Lower limb	Lower limb	Upper limb	Upper limb	Lower limb	Upper limb	Upper limb
Family history	Mother: MND	Father/sister: FTD	Mother: MND	None recorded	None recorded	None recorded	None recorded	None recorded	Sister had ALS
Cognitive assessment	ECAS – Not impaired	ECAS – Not impaired	ECAS – Not impaired	ECAS – Not impaired	ECAS – not done	ECAS – Not impaired	ECAS – not impaired	ECAS – not impaired	ECAS – not done
Genetics	*C9orf72*	*C9orf72*	*C9orf72*	No mutation	No mutation	No mutation	*p.I114T*	*p.I114T*	*p.I114T*
p62 staining	p62 in dentate gyrus, CA4 sector of hippocampus and granule cells of cerebellum	p62 in dentate gyrus, CA4 sector of hippocampus and granule cells of cerebellum	p62 in dentate gyrus, CA4 sector of hippocampus and granule cells of cerebellum	No significant p62 pathology	No significant p62 pathology	No significant p62 pathology	No significant p62 pathology	No significant p62 pathology	No significant p62 pathology

Table summarizing the clinical data associated with the cases implemented in the independent BaseScope validation of the hits identified by spatial transcriptomics.

proteasome, where the protein is degraded and the ubiquitin molecules recycled. There is evidence to suggest that mechanisms exist to prioritize the degradation of certain proteins over others by increasing the number of ubiquitin molecules attached to the protein [33]. The ability to either (i) reverse the fate of these ubiquitinated proteins, (ii) recycle ubiquitin molecules or (iii) prioritize specific proteins for degradation, relies upon the function of de-ubiquitinating proteins. USP47, found to exhibit lower expression in the cortex of our ALS cohort patients compared to controls, is one such de-ubiquitinating protein. De-ubiquitinating proteins can either fully remove a ubiquitin motif from a protein to prevent degradation, or remove only a part of it, to enable recycling of ubiquitin molecules and/or to allow for the prioritization of certain proteins by removing ubiquitin molecules from proteins with a less urgent need for degradation [33].

Expression of *USP47* was also found to be specifically increased in the granule cell layer of the cerebellum of patients with the *C9orf72* hexanucleotide repeat expansion compared to controls, but not in the cerebellum of patients with other causes of ALS (sporadic or *SOD1* mutation). The cerebellum of *C9orf72* ALS patients is also found to have a high burden of protein misfolding, particularly in the granule cell layer, where expression of *USP47* is found to be the greatest. There are, however, no clinical manifestations associated with this high burden of protein misfolding. This implies, that whilst there is clearly an underlying pathology, the cells are somehow able to cope without evidence of neurotoxicity seen in other similarly affected areas, such as the motor cortex. The finding that USP47 is increased in these cells could be associated with an increased capacity to recycle ubiquitin and prioritize toxic proteins, like TDP-43, for degradation. Indeed, the cells of the granule cell layer in *C9orf72* patients, whilst containing abundant p62 positive protein aggregates, rarely exhibit TDP-43 aggregation [32]. TDP-43 aggregation is seen in other brain regions and has been associated, through multiple neuropathological, *in vitro* and *in vivo* studies, with neurotoxicity therein [9]. It is therefore possible that increasing the expression of de-ubiquitinating proteins, such as USP47, may be a potential therapeutic strategy in ALS patients.

USP47 has also been shown to be directly involved in promoting cell survival through an anti-apoptotic mechanism mediated through its interaction with beta-

transducin repeats-containing protein (beta-TRCP; [34]). The observation, therefore, that *USP47* is upregulated in the cerebellum, where there is comparatively substantially less cell death, may be unrelated to its role in proteostasis, and may instead be related to its protective interaction with beta-TRCP. Furthermore, USP47 has been shown to play a crucial, regulatory role in axonal growth during development [35], therefore its reduced expression in the cortex could be associated with axonal dysfunction. Further mechanistic studies are clearly warranted to probe these regional differences further. However, de-ubiquitinating proteins are important drug targets in the oncology field, demonstrating good safety and efficacy profiles [33]. It is therefore possible that de-ubiquitinating enzymes (DUBs) could provide a potential therapeutic target in ALS.

Retaining spatial resolution

Our experiments demonstrated specific spatial localization of regionally distinct transcripts (Figure S1). Furthermore, our simulated whole-tissue evaluation was able to validate five out of fifteen previously identified dysregulated transcripts, that were independently validated by qPCR, from a whole-tissue analysis of *C9orf72* patient cerebellar tissue (Table S1; [36]). This implies that spatial transcriptomics is not only able to detect and replicate differences found in whole-tissue experiments, it also has the added benefit of being able to detect, more targeted, hypothesis driven and spatially resolved questions as implemented in our study. Using this approach, we were able to identify two spatially dysregulated transcripts that have previously eluded classical whole-tissue approaches.

Moreover, by firstly assessing cerebellar tissue, we were able to overcome previously identified issues regarding death and dying-cell artefact. In motor cortex and/or spinal cord, many transcripts are identified that may be a generic signature of dying cells, rather than a reflection of underlying pathology that could be driving the disease. By initially examining cerebellar tissue, we were able to analyse the transcriptome of cells that clearly have cellular pathology, including cytoplasmic protein inclusions, but are not undergoing cell death, and then validate candidate transcripts in other brain regions using a more targeted approach. Using this approach, we were able to demonstrate differential dysregulation of transcripts across distinct CNS regions, that may account for differential susceptibilities to the underlying disease process.

Study limitations

ST is a new technology that, to our knowledge, has never been used to interrogate human *post mortem* brain tissue. As with any novel technology there are limitations that must be taken into account when assessing the generated data. *Post mortem* brain tissue is subject to particularly high levels of autolysis compared to other tissues, which may compromise its RNA integrity. This technique is best implemented as a non-biased assessment of the spatial transcriptome. Clearly with tissue demonstrating substantial RNA degradation, there could be a bias towards the identification of more robust transcripts potentially skewing the data set. However, given these limitations, we implemented an extensive validation of potential hits using a much larger sample size (including both technical and biological replicates) and a technique that is not subject to the same degradation bias, BaseScope, which (i) can detect partially degraded mRNA and (ii) can be implemented on FFPE tissue, with better mRNA preservation compared to frozen tissue. New refinements in ST technology, such as sequential approaches and/or compilation of larger aligned data sets, may further extend the applications of this technology to the assessment of human neurodegenerative conditions [14,37].

Conclusions

Taken together these data indicate that through maintaining spatial resolution when assessing transcriptional dysregulation, it is possible to identify genes whose dysregulation may be contributing to the differential regional and cell-type specific susceptibility to disease and may shed light upon previously unidentified pathways contributing to the pathogenesis of ALS.

Acknowledgements

The authors would like to acknowledge the support and close collaboration with Joakim Lundeburg on this project. The Lundeburg lab kindly contributed laboratory expertise and troubleshooting advice and Joakim Lundeberg's comments were crucial in the manuscript

drafting process. The authors would also like to thank (i) the MRC Edinburgh Brain Bank for supplying all *post mortem* brain material and the Scottish MND Register/CARE-MND Consortium for all clinical and demographic data. (ii) The Scottish MND Clinical Specialist, team in discussing and obtaining consent from MND patients for inclusion in these resources. (iii) MND Scotland and the Sylvia Aitken Charitable Trust for funding CS to help to establish the MND Tissue bank (iv) we acknowledge funding from the UK Medical Research Council and Engineering and Physical Sciences Research Council to the Edinburgh/St Andrews Molecular Pathology Node and funding from BioGen to JMG. JMG is also funded by a starter grant for clinical lecturers from the AMS (210JMG 3102 R45620) and brain bank funding is from the MRC (MR/L016400/1).

Author contributions

JG, MRL, SC, CS and TA contributed to (i) the conception and design of the study, (ii) acquisition and analysis of data and (iii) drafting a significant portion of the manuscript or figures. KM, IC and SMP contributed to (i) the conception and design of the study, (ii) acquisition and analysis of data.

Conflicts of interest

The authors declare no other conflicts of interest. The Editors of Neuropathology and Applied Neurobiology are committed to peer-review integrity and upholding the highest standards of review. As such, this article was peer-reviewed by independent, anonymous expert referees, and the authors (including CS) had no role in either the editorial decision or the handling of the paper.

References

1 Corcia P, Couratier P, Blasco H, Andres CR, Beltran S, Meininger V, *et al*. Genetics of amyotrophic lateral sclerosis. *Rev Neurol* 2017; **173**: 254–262
2 Mathis S, Goizet C, Soulages A, Vallat JM, Masson GL. Genetics of amyotrophic lateral sclerosis: a review. *J Neurol Sci* 2019; **15**: 217–226
3 DeJesus-Hernandez M, Mackenzie IR, Boeve BF, Boxer AL, Baker M, Rutherford NJ, *et al*. Expanded GGGGCC hexanucleotide repeat in noncoding region of C9ORF72 causes chromosome 9p-linked FTD and ALS. *Neuron* 2011; **20**: 245–56
4 Renton AE, Majounie E, Waite A, Simón-Sánchez J, Rollinson S, Gibbs JR, *et al*. A hexanucleotide repeat expansion in C9ORF72 is the cause of chromosome 9p21-linked ALS-FTD. *Neuron* 2011 **20**: 257–68
5 Ash PE, Bieniek KF, Gendron TF, Caulfield T, Lin WL, Dejesus-Hernandez M, *et al*. Unconventional translation of C9ORF72 GGGGCC expansion generates insoluble polypeptides specific to c9FTD/ALS. *Neuron* 2013; **20**: 639–46
6 Reddy K, Zamiri B, Stanley SY, Macgregor RB Jr, Pearson CE. The disease-associated r(GGGGCC)n repeat from the C9orf72 gene forms tract length-dependent uni- and multimolecular RNA G-quadruplex structures. *J Biol Chem* 2013; **5**: 9860–6
7 Ciura S, Lattante S, Le Ber I, Latouche M, Tostivint H, Brice A, *et al*. Loss of function of C9orf72 causes motor deficits in a zebrafish model of amyotrophic lateral sclerosis. *Ann Neurol* 2013; **74**: 180–7
8 Devenney E, Foxe D, Dobson-Stone C, Kwok JB, Kiernan MC, Hodges JR. Clinical heterogeneity of the C9orf72 genetic mutation in frontotemporal dementia. *Neurocase* 2015; **21**: 535–41
9 Taylor JP, Brown RH Jr, Cleveland DW. Decoding ALS: from genes to mechanism. *Nature* 2016; **10**: 197–206
10 Neumann M, Sampathu DM, Kwong LK, Truax AC, Micsenyi MC, Chou TT, *et al*. (2006) Ubiquitinated TDP-43 in frontotemporal lobar degeneration and amyotrophic lateral sclerosis. *Science* 2006; **6**: 130–3
11 Ince PG, Highley JR, Kirby J, Wharton SB, Takahashi H, Strong MJ, *et al*. Molecular pathology and genetic advances in amyotrophic lateral sclerosis: an emerging molecular pathway and the significance of glial pathology. *Acta Neuropathol* 2011; **122**: 657–71
12 Ravits J, Appel S, Baloh RH, Barohn R, Brooks BR, Elman L, *et al*. Deciphering amyotrophic lateral sclerosis: what phenotype, neuropathology and genetics are telling us about pathogenesis. *Amyotroph Lateral Scler Frontotemporal Degener* 2013; **14**(Suppl. 1): 5–18.
13 Ståhl PL, Salmén F, Vickovic S, Lundmark A, Navarro JF, Magnusson J, *et al*. Visualisation and analysis of gene expression in tissue sections by spatial transcriptomics. *Science* 2016; **1**: 78–82
14 Maniatis S, Äijö T, Vickovic S, Braine C, Kang K, Mollbrink A, *et al*. Spatiotemporal dynamics of molecular pathology in amyotrophic lateral sclerosis. *Science* 2019; **5**: 89–93
15 Ferreira PG, Muñoz-Aguirre M, Reverter F, Sá Godinho CP, Sousa A, Amadoz A, *et al*. The effects of death and post-mortem cold ischemia on human tissue transcriptomes. *Nat Commun* 2018; **13**: 490
16 Al-Sarraj S, King A, Troakes C, Smith B, Maekawa S, Bodi I, *et al*. p62 positive, TDP-43 negative, neuronal cytoplasmic and intranuclear inclusions in the cerebellum and hippocampus define the pathology of

C9orf72-linked FTLD and MND/ALS. *Acta Neuropathol* 2011; **122**: 691–702
17 Wang F, Flanagan J, Su N, Wang LC, Bui S, Nielson A, *et al*. RNAscope: a novel in situ RNA analysis platform for formalin-fixed, paraffin-embedded tissues. *J Mol Diagn* 2012; **14**: 22–9
18 Navarro JF, Sjöstrand J, Salmén F, Lundeberg J, Ståhl PL. ST Pipeline: an automated pipeline for spatial mapping of unique transcripts. *Bioinformatics* 2017; **15**: 2591–2593
19 Ebbert MTW, Ross CA, Pregent LJ, Lank RJ, Zhang C, Katzman RB, *et al*. Conserved DNA methylation combined with differential frontal cortex and cerebellar expression distinguishes C9orf72-associated and sporadic ALS, and implicates SERPINA1 in disease. *Acta Neuropathol* 2017; **134**: 715–728
20 Harrison PJ, Lyon L, Sartorius LJ, Burnet PW, Lane TA. The group II metabotropic glutamate receptor 3 (mGluR3, mGlu3, GRM3): expression, function and involvement in schizophrenia. *J Psychopharmacol* 2008; **22**: 308–22
21 Cozzi A, Attucci S, Peruginelli F, Marinozzi M, Luneia R, Pellicciari R, *et al*. Type 2 metabotropic glutamate (mGlu) receptors tonically inhibit transmitter release in rat caudate nucleus: in vivo studies with (2S,1'S,2'S,3'R)-2-(2'-carboxy-3'-phenylcyclopropyl) glycine, a new potent and selective antagonist. *Eur J Neurosci* 1997; **9**: 1350–5
22 Battaglia G, Monn JA, Schoepp DD. In vivo inhibition of veratridine-evoked release of striatal excitatory amino acids by the group IImetabotropic glutamate receptor agonist LY354740 in rats. *Neurosci Lett* 1997; **229**: 161–4
23 Lovinger DM, McCool BA. Metabotropic glutamate receptor-mediated presynaptic depression at corticostriatal synapses involves mGLuR2 or 3. *J Neurophysiol* 1995; **73**: 1076–83
24 Cartmell J, Schoepp DD. Regulation of neurotransmitter release by metabotropic glutamate receptors. *J Neurochem* 2000; **75**: 889–907
25 Corti C, Battaglia G, Molinaro G, Riozzi B, Pittaluga A, Corsi M, *et al*. The use of knock-out mice unravels distinct roles for mGlu2 and mGlu3 metabotropic glutamatereceptors in mechanisms of neurodegeneration/neuroprotection. *J Neurosci* 2007; **27**: 8297–308
26 Battaglia G, Riozzi B, Bucci D, Di Menna L, Molinaro G, Pallottino S, *et al*. Activation of mGlu3 metabotropic glutamate receptors enhances GDNF and GLT-1 formation in the spinal cord and rescues motor neurons in the SOD-1 mouse model of amyotrophic lateralsclerosis. *Neurobiol Dis* 2015; **74**: 126–36. https://doi.org/10.1016/j.nbd.2014.11.012. Epub 2014 Nov 28
27 Ghose S, Gleason KA, Potts BW, Lewis-Amezcua K, Tamminga CA. Differential expression of metabotropic glutamate receptors 2 and 3 in schizophrenia: a mechanism for antipsychotic drug action? *Am J Psychiatry* 2009; **166**: 812–20. https://doi.org/10.1176/appi.ajp.2009.08091445. Epub 2009 Jun 1
28 García-Bea A, Bermudez I, Harrison PJ, Lane TA. A group II metabotropic glutamate receptor 3 (mGlu3, GRM3) isoform implicated in schizophrenia interacts with canonical mGlu3 and reduces ligand binding. *J Psychopharmacol* 2017; **31**: 1519–1526
29 O'Brien M, Burke T, Heverin M, Vajda A, McLaughlin R, Gibbons J, *et al*. Clustering of neuropsychiatric disease in first-degree and second-degree relatives of patients with amyotrophic lateral sclerosis. *JAMA Neurol* 2017; **74**: 1425–1430
30 Woolley ML, Pemberton DJ, Bate S, Corti C, Jones DN. The mGlu2 but not the mGlu3 receptor mediates the actions of the mGluR2/3 agonist, LY379268, in mouse models predictive of antipsychotic activity. *Psychopharmacology* 2008; **196**: 431–40
31 Fujioka R, Nii T, Iwaki A, Shibata A, Ito I, Kitaichi K, *et al*. Comprehensive behavioral study of mGluR3 knockout mice: implication in schizophrenia related endophenotypes. *Molecular Brain* 2014; **7**: 31
32 Mackenzie IR, Frick P, Neumann M. The neuropathology associated with repeat expansions in the C9ORF72 gene. *Acta Neuropathol* 2014; **127**: 347–57
33 Ao N, Chen Q, Liu G. The small molecules targeting ubiquitin-proteasome system for cancer therapy. *Comb Chem High Throughput Screen* 2017; **20**: 403–413
34 Peschiaroli A, Skaar JR, Pagano M, Melino G. The ubiquitin-specific protease USP47 is a novel beta-TRCP interactor regulating cell survival. *Oncogene* 2010; **29**: 1384–93
35 Yang SW, Oh KH, Park E, Chang HM, Park JM, Seong MW, *et al*. USP47 and C terminus of Hsp70-interacting protein (CHIP) antagonistically regulate kataninp60-mediated axonal growth. *J Neurosci* 2013; **33**: 12728–12738.
36 Prudencio M, Belzil VV, Batra R, Ross CA, Gendron TF, Pregent LJ, *et al*. Distinct brain transcriptome profiles in C9orf72-associated and sporadic ALS. *Nat Neurosci* 2015; **18**: 1175–82
37 Eng CL, Lawson M, Zhu Q, Dries R, Koulena N, Takei Y, *et al*. Transcriptome-scale super-resolved imaging in tissues by RNA seqFISH. *Nature* 2019; **568**: 235–239

Supporting information

Additional Supporting Information may be found in the online version of this article at the publisher's web-site:

Table S1. Simulated whole-tissue experiment validates previous transcriptomic data sets from *C9orf72* cerebellum

Table S2. Summary of QC data from spatial transcriptomics sequencing. Table summarizing the QC data from the spatial transcriptomics sequencing. CF1 and CF2 refer to the control sections and ME2 refers to the motor neurone disease section

Figure S1. Expression heat map shows localized expression of candidate transcripts demonstrating regional specificity of ST.

Figure S2. Six transcripts identified as differentially expressed by ST showed no difference when assessed by BaseScope in the same ALS case and control.

Figure S3. Expression of positive (*PPIB*) and negative (*DapB*) control probes across all cases shows no statistically significant difference in RNA quantity or quality between cases assessed in our cohort

Received 20 August 2019
Accepted after revision 21 December 2019
Published online Article Accepted on 10 January 2020